Publisher homepage: www.universepg.com, ISSN: 2707-4625 (Online) & 2707-4617 (Print)

https://doi.org/10.34104/ijmms.022.075082

International Journal of Material and Mathematical Sciences

Journal homepage: www.universepg.com/journal/ijmms

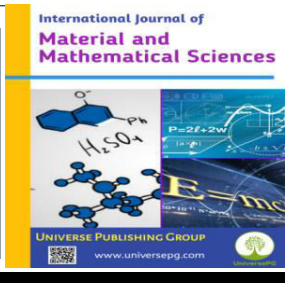

Synthesis of Titanium Dioxide by Sol-Gel Method and Comparison with Titanium Dioxide Pure

Yasmin Abd Elrazeg[1]*, Md. Badiruzzaman[2], Mazharul Islam[3], Md. Mahbub Morshed[4], and Ahmed A. Elmugdad[1]

[1]College of Science, Dept. of Chemistry, Sudan University of Science & Technology, Sudan and [2]Dept. of Biochemistry and Molecular Biology, University of Dhaka, Bangladesh; and [3]Dept. of Chemistry, Shahjalal University of Science and Technology, Bangladesh; and [4]Dept. of Biotechnology and Genetic Engineering Mawlana Bhashani Science and Technology University, Bangladesh.

*Correspondence: yasabao01@gmail.com (Yasmin Abd Elrazeg, College of Science, Dept. of Chemistry, Sudan University of Science & Technology, Sudan).

ABSTRACT

This paper study the synthesis of the TiO_2 nanoparticles using the sol-gel method and $TiCl_4$ as raw material (TiO_2 sol-gel) and characterize it and TiO_2 pure by Powder X-Ray Diffraction (XRD), both samples show they are anatase phase with high crystallinity and purity. Fourier transform infrared spectrum (FTIR) both samples it showed in the graph that TiO_2 pure, TiO_2 sol-gel various frequency vibrations which are shown by different peaks formed, The specific surface area and porosity of the TiO_2 pure (46.962 m^2/g) and TiO_2 sol-gel (38.264 m^2/g) were evaluated by using the nitrogen adsorption and desorption isotherms by using Brunauer-Emmett-Teller (BET) method. Using Ocean Optio USB- 2000 spectrometer for optical properties which are related to the absorption spectrum but using diffuse reflectance spectrum in state of the Kubelka-Munk remission function replaces the Lambert-Beer law.

Keywords: Sol-gel method, Ocean Optio USB-2000 spectrometer, and Diffuse reflectance spectrum.

INTRODUCTION:

Nanotechnology is a broad and intense area of research and development that has been growing worldwide in the past decade. Nano-materials are substances whose dimension is less than approximately 100 nanometers (Hayle, 2014). Nanocrystalline semiconductors have achieved great importance in the industrial world today (Wang, 2010; Qu, 2013) which include metal oxides (ZnO, V_2O_5, Fe_2O_3, SnO_2, CdO, and TiO_2) and metal sulphide (CdS and ZnS) (Karunakaran, 2004). Titanium dioxide is an important semiconductor material due to its properties such as cheap, nontoxic, photo-chemical and chemical stability, high refractive index, wide band gap (Cassano, 2000; Wang, 2010). Soit was applied in environmental protection, paint, toothpaste, UV protection, photo-catalysis, photo-voltaic's, electrochromics, gas sensing, dye-sensitized solar cells, photo-induced hyrophilicity, and soon (Liu, 2007; Chen, 2006; 2012; Ohenoja, 2013). Titanium dioxide crystallized in four natural phases: brookite (orthorhombic), anatase (tetragonal), rutile (tetragonol) and TiO_2 (B) (monoclinic). The three crystal structures of TiO_2 are shown in **Fig. 1**. Besides these polymorphs two additional high- pressure forms have been synthesized from rutile; the first form is TiO_2 (II) with a PdO_2 structure (Simons, 1967) and the second form is TiO_2 (H) with a hollandite structure (Latroche, 1989; Yousif and Ali, 2021).

Among the titanium dioxide forms rutile phase is the most thermodynamically stable whereas brookite are transformed to rutile on heating (Ohenoja, 2013). Various investigations have established that TiO_2 is much more effective as a photo-catalyst in the form of nanoparticles than in bulk powder. During the past two decades, several synthetic methods have been used to prepare TiO_2 nanoparticles (Su, 2006).

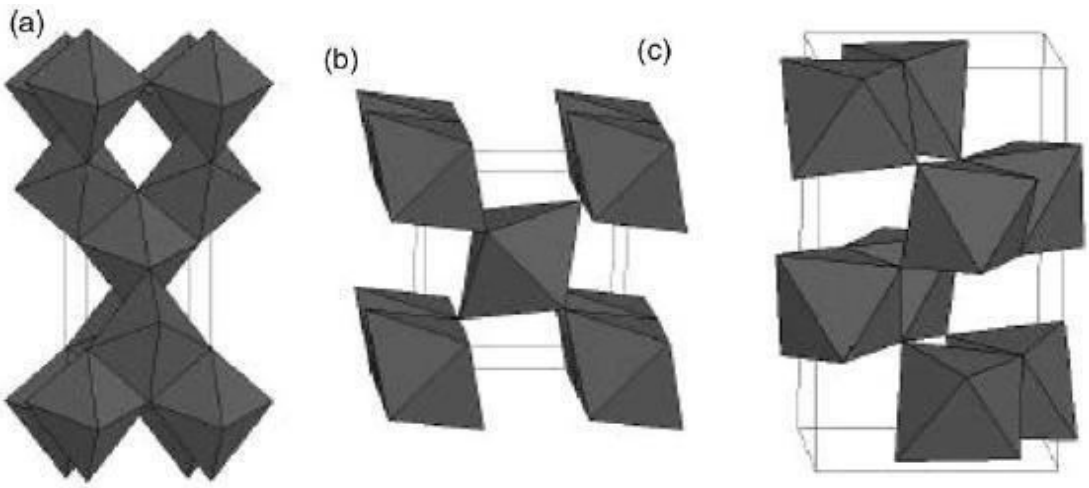

Fig. 1: Crystal structures of (a) TiO_2anatase, (b) brookite, and (c) rutile.

Generally, the methods of preparing nano-TiO_2 are gas methods (chemical vapor deposition CVD, physical vapor deposition PVD and spray pyrolysis) and liquid methods (co-precipitation, solvothermal, microemulsion, combustion synthesis, electrochemical synthesis, sol-gel methods) (Carp, 2004).

Liquid methods are often used because they do not need any special equipment in comparison with gas methods (Chen, 2006). Properties of nano-TiO_2 particles are dependent on synthesis method which is responsible for their chemical purity and its crystal form (anatase or rutile) also on various particle features (specific surface area and particle size), crystallinity and surface chemistry (Carp, 2004). Among these methods, sol-gel method is regarded as good method for synthesis ultra-fine metallic oxide and has been widely employed for preparing titanium dioxide nanoparticles (Su, 2006).

The sol-gel method has many advantages such as purity, stoichiometry control, ease of processing, and control over composition (Carp, 2004). The usually sol-gel procedure includes three steps; hydrolysis, drying, and calculation. There are two types of titanium sources for preparation of nano-TiO_2 particles which include organic titanium alkoxide (titanium iso-propoxide $Ti(i\text{-}OP)_4$, Titanium ethoxide $Ti(OE)_4$, etc.) and inorganic titanate (titanium tetrachloride $TiCl_4$, titanium trichloride $TiCl_3$ or Titanium sulphate $TiO(SO_4)_2$) (Carp, 2004). When using Titanium alkoxide expensive chemicals must be used and the hydrolysis process is difficult to control; otherwise, tetrachloride $TiCl_4$ is cheap, easy control of hydrolysis (Zhu, 2000; Chen, 2006). Titanium dioxide has been prepared in different morphologies powder, thin film, annotates and nanorods (Burda, 2005; Banu *et al*., 2021).

The sol-gel method was used for the syn-thesis titanium dioxide nano particle with using titanium tetrachloride as a precursor. And study its and titanium dioxide pure properties by using X-Ray Diffraction (XRD), micrometric gas adsorption analyzer by using Brunauer-Emmett-Teller (BET) method, Ocean Optic-USB-2000 spectrometer.

MATERIALS AND METHODS:

Pure Titanium dioxide from Aldrich, Titanium tetrachloride $TiCl_4$ (M_{wt} 189.87gmol-1, 99.9%), absolute Ethanol, Ammonium hydroxide (M_{wt} 17.03gmol-1, 25%), di-ionized water, silver nitrate (M_{wt} 169.87 gmol-1, 98.4%).

Preparation catalyst

A sample of titanium dioxide nanoparticles was synthesized by using the Sol-gel method, 30cm^3 of titanium tetra chloride was added to 500 cm^3 di-ionized water in an ice bath under fume-hood followed by the addition 350 cm3 of ethanol with vigorous stirring for half of the hour at room temperature. Justified the pH to 8 by adding ammonia solution 25% drop by drop and precipitate was obtained.

After stirring vigorously then the solution was made to settle for 24 hours. Then the precipitate was separated by using a centrifuge and washed to remove chloride ions using silver nitrate to detect that then the precipitate was dried at 200^oC for two hours and an amorphous TiO_2 was obtained. At last obtainned the powder of titanium di-oxide nanoparticles (Uddin *et al*., 2021; Hayle, 2014)

Methods of Characterization of TiO_2 Nanomaterials

There are many methods to characterize TiO_2 nanomaterial. In this study used X-ray powder diffraction (XRD) was performed using PAN-alytical's X-ray diffract meter (Cu X-ray λ = 1.540598Å) over a range (10-60)° 2θ the powdered sample was packed on the sample holder by back pressure technique and mounted on the sample stage of the machine then determination the particles structure crystal size from the XRD pattern.

The crystallite sizes of the TiO2 nano-materials were estimated using Scherer equation (1) (Han, 2012; Hayle, 2014).

$$\mathbf{d}=\frac{\lambda K}{\beta \cos\theta} \qquad (1)$$

Where d is the crystallite size in nanometer, K is the shape factor constant, which is 0.89, β is the full width at half maximum (FWHM) in radian, λ is the wave length of the X-ray which is 0.1540598nm for Cutarge tKα radiation and is the Bragg angle, Micrometric gas adsorption analyzer.

The specific surface area and porosity of the two samples were evaluated by using the nitrogen pressure sata constant temperature (typically liquid N2, 77K) the sample loaded (0.1036g of sample 1, 0.60 98g of sample 2) (Analysis Time is 281.6 min for sample 1,571.2 min for sample 2) then nitrogen adsorption isotherm of both samples were analyzed for the specific surface area using the BET equation (3) which required a linear plot of1/[W(P/P0)-1] against P/P0.

$$slope = \frac{C-1}{W_m C}, Intercept = \frac{1}{W_m C} \quad (2)$$

$$\frac{1}{W((P_0/P)-1)} = \frac{1}{W_m C} + \frac{C-1}{W_m C}\left(\frac{P}{P_0}\right) \quad (3)$$

Where W = weight of gas adsorbed, P/P0 =relative pressure, Wm = weight of adsorbate as monolayer, C = BET constant. Using FTIR-8400S Fourier transform infrared spectroscopy to analyzed the both samples.

The samples were grind down with KBr and press to make disk and insert into the sample holder then take the FTIR spectra in range (400 – 3000cm-1).

Ocean optio USB2000 Spectrometer stat up by connect it to desktop PC via USB port or serial port, Ocean Optics OOI Base32 software application installed and configured for use with the USB 2000 OOIBase32 can use to get spectroscopic measurements (such as absorbance, reflectance, and emission) .

At first stored reference and dark measurements then the light transmits through an optical fiber to the sample. There is another optical fiber collects and transmits the result of the interaction to the spectrometer, then OOIBase32 compares the sample to the reference measurement and displays the spectral information. In reflectance spectroscopy, the Kubelka-Munk remission function F(R) replaces the Lambert-Beer law (Sikorska, 2003).

$$F(R)=\frac{(1-R)^2}{2R}=\frac{K}{S} \quad (4)$$

RESULTS AND DISCUSSION:

Sol-gel TiO2 catalyst

When $TiCl_4$ solution was added to two of di-ionized water under fume hood, an exothermic reaction was observed. Then, a white precipitate was obtained after adding a drop of ammonium hydroxide (NH_4OH) wisely; and the yellow gel rose this indicates the formation of $Ti(OH)_4$.

After stirring the solution settling and centrifuging and drying the precipitate which leads to the formation of white amorphous TiO_2; then cooling, grinding and calcination lead to the form-ation of white powder TiO_2 nanoparticles. The Weight of precipitate before calcimined is 19.2005g. The weight of precipitate after calcinated is 14.4458g.

Characterization of the catalysts

As can be observed from **Fig. (1** and **2)**, the XRD peaks in the angle range of 20°< 2θ° < 60° for TiO_2 (pure) which are 25.4039°, 36.9877°, 37.8628°, 38.6280°, 48.0839°, 53.9365° and 55.1030°an for TiO_2(sol-gel) which are 25.3275°, 37.8174°, 48.

0607°, 53.8852°, and 55.0714° among the XRD peaks. The width of 25.4039° for TiO_2 (pure) and 25.3275° for TiO_2 (sol-gel) are useful peak since they have a high intensity which in turn are used to determine crystals size. According to (Hayle, 2014) the peaks values correspond to the tetragonal anatase phase. Using equation (1) the estimated crystalline size is explored in the following table.

Table 1: Crystallite size (d) of pure TiO_2 & sol-gel TiO2nano-materials.

Sample	20°	FWHM radians	Crystalline size Nm
TiO_2(pure)	25.4039	0.0030908	49.11070
TiO_2(sol-gel)	25.0819	0.0068696	22.08194

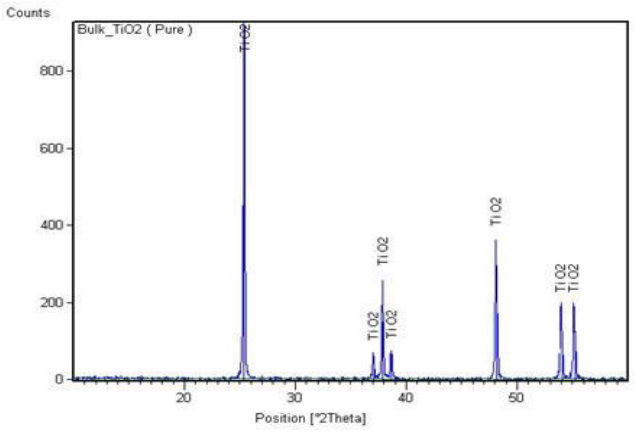

Fig. 1: The XRD pattern of TiO_2 (pure).

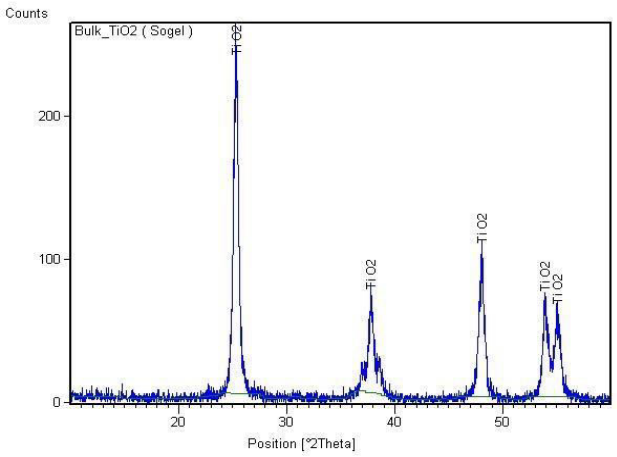

Fig. 2: The XRD pattern of TiO_2 (sol- gel).

A sharp increase in adsorption volume of $N_2$was observed and located in the P/Po range of (0.067 - 0.88), (0.36 – 0.89) for TiO_2 pure and TiO_2 sol-gel respectively. The specific surface area value of the TiO_2 pure is 46.962 m²/g and the specific surface area value of the TiO_2 sol-gel is 38.264 m²/g (Govindaraj, 2015).

Micrometric gas adsorption analyzer

Fig. (3a, b) is shown the nitrogen adsorption and desorption isotherm which exhibits a type IV pattern with hysteresis loop characteristic of mesoporous material according to the classification of IUPAC.

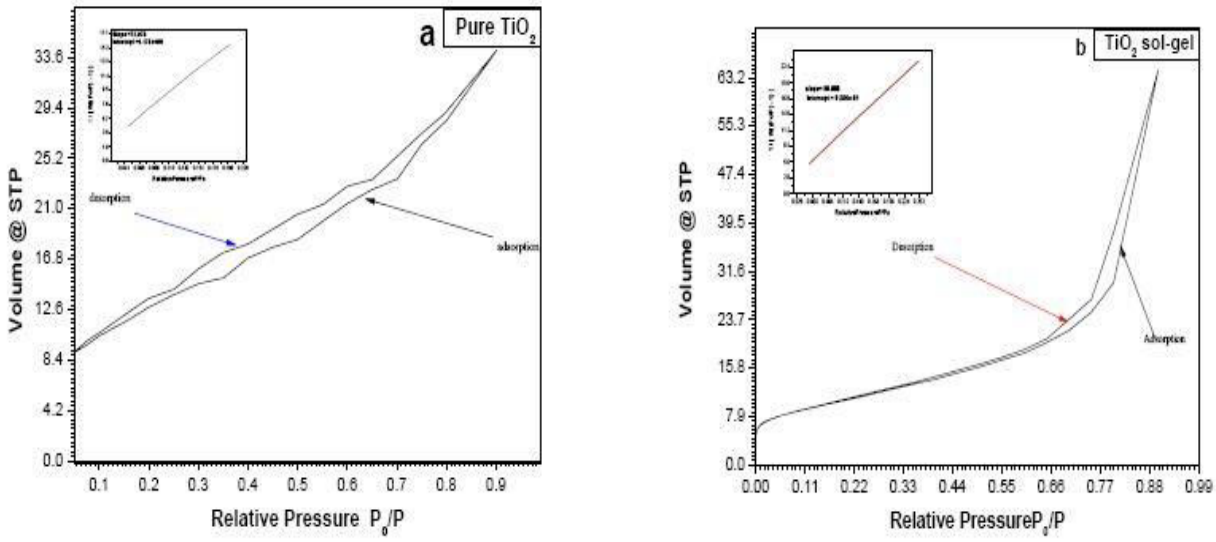

Fig. 3: a. Nitrogen Adsorption-Desorption isotherm of pure TiO_2 b. Nitrogen Adsorption-Desorption isotherm of TiO_2sol-gel.

Fourier transforms infrared (FTIR) spectroscopy

In this graph different peaks formed at different wave numbers (400-3000cm^{-1}). It is noticed that TiO_2 pure, TiO_2 sol-gel various frequency vibrations which are shown by different peaks formed. The peak in the range (400 – 800cm^{-1}) was characteristic Ti-O. The peak in range 1426-1696cm-1 was characteristic of the O-Ti-O bond and Ti= =O bending region. In **Fig. 4b** there is the peak in the range (2000-3000) is characteristic O-H (Grujić, 2006).

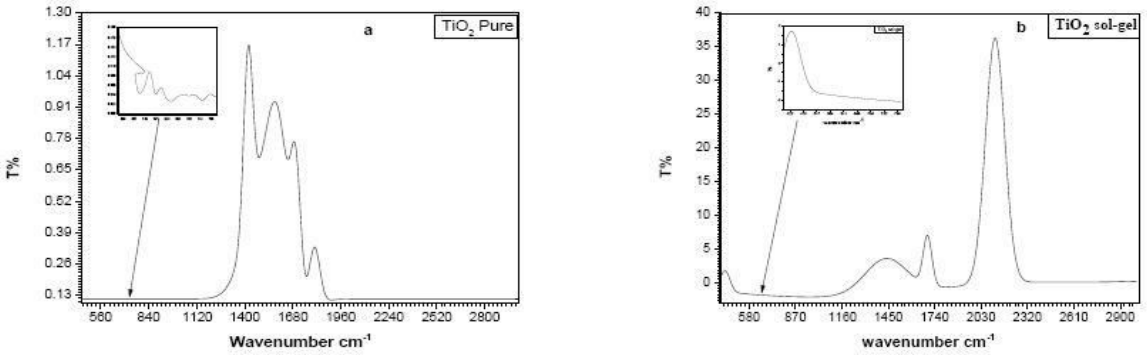

Fig. 4: (a). The FTIR spectra of TiO_2 pure; (b). The FTIR spectra of TiO_2 sol-gel.

Optical properties using USB 2000 spectrometer

Fig. 5 displays the reflectance spectra of TiO_2 pure which has a maximum value at region (371-408nm), (483- 506nm) and above 650nm. We noticed the reflectance spectrum is decreased in region (410-629). The reflectance spectra of TiO_2 sol-gel it. Has a maximum value at region (373-694nm) the curve s reach's saturation above 669nm.We noticed the reflectance spectra are decreased in the region (520-540nm),(576 - 584) and (657- 690nm).

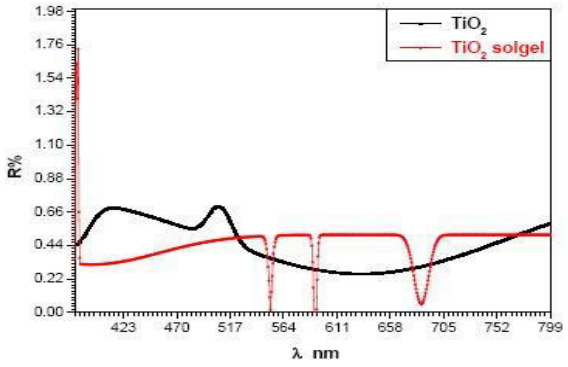

Fig. 5: The reflectance spectra of (TiO_2pure) and TiO_2sol-gel.

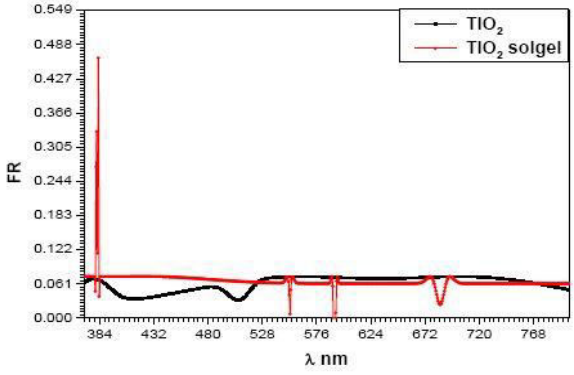

Fig. 6: Diffuse reflectance spectrum of TiO_2 pure and TiO2 sol-gel with Kubelka-Monk conversion.

The optical absorption coefficient, α, which is the relative rate of decrease in light intensity along its path of propagation, was calculated using equation (5) from the transmittance and reflectance data in the wavelength range 300-800nm. The nature of the optically induced transitions was determined from these data (Baydogan, 2013; and Rabeh, 2014).

$$\alpha(h\nu) = \frac{1}{d}\left[\frac{(1-R)^2}{T}\right] \quad (5)$$

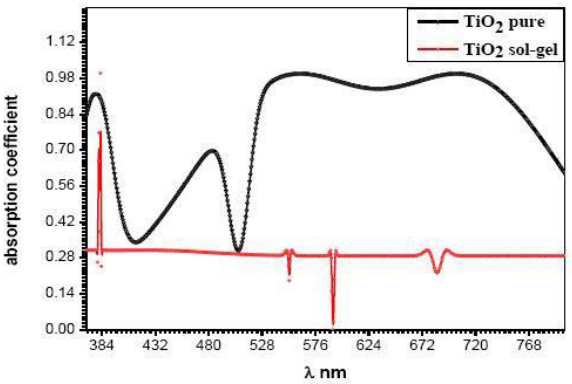

Fig. 7: The optical absorption coefficient of TiO_2 pure and TiO_2sol-gel.

Where T is the transmittance, R is the reflectance, and d is the sample thickness. The optical absorption coefficient was found to be exponentially dependent on the photon energy. However, when the particle size decreases the optical absorption coefficient will increase **Fig.7** show that TiO_2 sol-gel has a high value of 0.99 at 384nm and TiO_2 pure has 0.92 at 379nm.

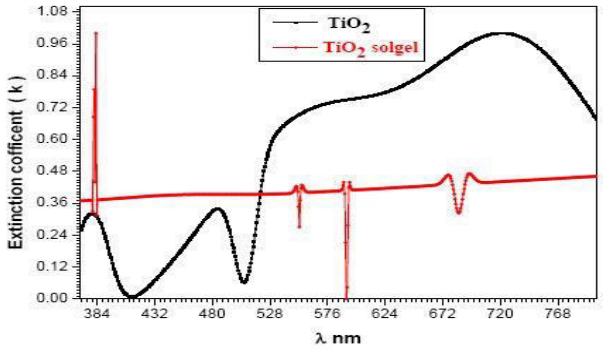

Fig. 8: The extinction coefficient TiO_2 pure and TiO_2sol-gel.

The extinction coefficient which is shown in **Fig. 8** was calculated using equation (6)

$$k = \frac{\alpha\lambda}{4\pi} \quad (6)$$

Where k is the extinction coefficient, α is the absorption co-efficient and λ is the wavelength. The difference in values of extinction coefficient for two samples TiO_2 pure (0.32), and TiO_2 sol-gel due to that TiO_2 sol-gel has a small particle size. The refractive index determined using transmittance and reflectance measurements from **Fig. 9** is noticed that there refractive index has a maximum value of 11 at wavelength 415 nm for TiO_2 pure and 16.3 at wavelength 384 nm for TiO_2 sol-gel which is due to interactions takes place between photons and electrons. The refractive index changes with the variety of the wavelength of the incident light beam due to these interactions, i.e. the optical loss caused by absorption and scattering (Baydogan, 2013).

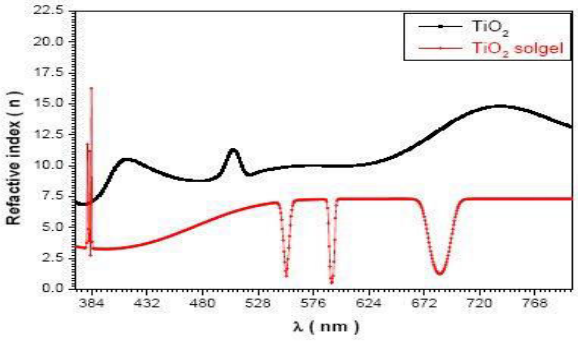

Fig. 9: The refractive index of TiO_2 pure and TiO_2sol-gel.

The energy band gap of these materials is determined using the reflection spectra. According to the Tauccrelation, the absorption coefficient is given by Sharma equation (7) (Rabeh, 2014).

$$\alpha(h\nu) = (B - E_g)^n \quad (7)$$

Where Eg is the energy gap, B constant is different for different transitions, (hν) is the energy of photon and n is an index which expects the values 1/2, 3/2, 2, and 3 depending on the nature of the electronic transition responsible for the reflection. The exponent r = 1/2, 3/2 for indirect transition is allowed or forbidden in the quantum mechanical sense, and r=2, 3 for allowed and forbidden direct transition, respectively. From **Fig. 10** the energy band gap is 3.07 eV for TiO_2 pure and 3.23 for TiO_2 sol-gel (Baydogan, 2013; Rabeh, 2014).

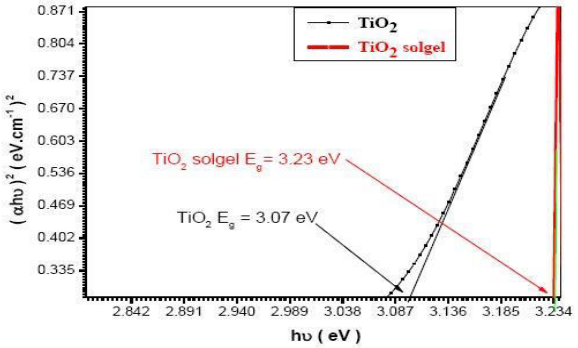

Fig. 10: The optical energy gab spectrum for TiO_2 pure and TiO_2sol-gel.

CONCLUSION:

TiO_2 nanomaterial was prepared by using the most convenient ways of synthesizing method known as sol gel synthesis. Sol-gel is and easy method due to low cost and is done at low temperature. XRD results exhibited the interesting peak value are (25. 4039°, 25.3275°) which is anatase TiO_2 nano- material due to (49.11070, 22.08194nm) for TiO_2 pure and TiO_2 sol-gel respectively. The specific surface area and porosity of theTiO_2 pure and TiO_2 sol-gel were evaluated by using the nitrogen adsorption and desorption isotherms, the specific surface area of the TiO_2 pure are 46.962 m²/g and The specific surface area of the TiO_2 sol-gel are38.264 m²/g. The isotherm exhibits a type IV pattern with a hysteresis loop. From the FTIR spectrum both samples observed that TiO_2 pure, TiO_2 sol-gel various frequency vibrations which are shown by different peaks formed. Optical properties are studied by using the Diffuse reflectance spectrum in which the Kubelka - Munk remission function replaces the Lambert-Beer law. TiO_2sol-gel has an optical absorption co-efficient (0.99), extinction coefficient (1), a refractive index 16.3 and the energy band gap of 3.23eV while TiO2 pure has optical absorption coefficient of 0.92, extincttion coefficient (0.32), there refractive index 11 and the energy band gap 3.03eV.

ACKNOWLEDGMENT:

Express gratitude to all who encouragement and helping. Thank Industrial Research and Consulting Center and especially thank Dr. Abd Elsakhi for his help.

CONFLICTS OF INTEREST:

The authors declare that the manuscript has no competing interests to the publication.

REFERENCES:

1) Banu MS, Raju I, and Mondal S. (2021). A comparative study on classical fourth order and butcher sixth order Runge-Kutta methods with initial and boundary value problems, *Int. J. Mat. Math. Sci*., **3**(1), 8-21. https://doi.org/10.34104/ijmms.021.08021
2) Baydogan, N., Ozdurmusoglu, T., Cimenoglu, H., Tugrul, A.B., (2013). Refractive Index and Extinction Coefficient of ZnO: Al Thin Films Derived by Sol-Gel Dip Coating Technique. *Defect and Diffusion Forum*, 334–335, 290–293. https://doi.org/10.4028/www.scientific.net/ddf.334-335.290
3) Burda, C., Chen, X., Narayanan, R. and El-Sayed, M.A., (2005). Chemistry and properties of nano crystals of different shapes. *Chemical reviews*, **105**(4), pp.1025-1102. https://doi.org/10.1021/cr030063a
4) Carp, O., Huisman, C.L. and Reller, A., (2004). Photo induced reactivity of titanium dioxide. *Progressin solid statec hemistry*, **32**(1-2), pp. 33-177. https://doi.org/10.1016/j.progsolidstchem.2004.08.001
5) Cassaignon, S., Koelsch, M. and Jolivet, J. P., 2007. From TiCl3 to TiO2 nanoparticles (anatase, brookite and rutile): Thermohydrolysis and oxidation in aqueous medium. *J. of Physics and Chemistry of Solids*, **68**(5-6), pp.695-700. https://doi.org/10.1016/j.jpcs.2007.02.020
6) Cassano, A.E. and Alfano, O.M., (2000). Reaction engineering of suspended solid heterogeneous photo catalyticreactors. *Catalysistoday*, **58**(2-3), pp.167-197. https://doi.org/10.1016/S0920-5861(00)00251-0
7) Chen, Y., Lin, A. and Gan, F., (2006). Preparation of nano-TiO2 from TiCl4 by dialysis hydrolysis. *Powder Technology*, **167**(3), pp.109-116. https://doi.org/10.1016/j.powtec.2006.06.015
8) Chen, J., Wang, H., Wei, X. and Zhu, L., (2012). Characterization, properties and catalytic application of TiO2 nano tubes prepared by ultrasonic- assistedsol - hydrothermal method. *Materials Research Bulletin*, **47**(11), pp.3747-3752. https://doi.org/10.1016/j.materresbull.2012.06.029
9) Govindaraj, R., Pandian, M.S., and Mukhopadhyay, S., (2015). Synthesis of poroustitanium dioxidenanorods / nanoparticles and their properties for dye sensitized solar cells. *Journal of Materials Science: Materials in Electronics*, **26**(4), pp.2609-2613. https://doi.org/10.1007/s10854-015-2731-y
10) Grujić-Brojčin, M., Šćepanović, M., Dohčević-Mitrović, Z. (2006). Infrared Study of Non-stoichiometric Anatase TiO2 Nano powders. *Science of Sintering*, **38**(2). https://doi.org/10.2298/SOS0602183G
11) Han, H. and Bai, R., (2009). Buoyant photocatalyst with greatly enhanced visible-light activity prepared through a low temperature hydro thermal method. *Industrial & Engineering Chemistry Research*, **48**(6), pp.2891-2898. https://doi.org/10.1021/ie801362a
12) Hayle, S.T. and Gonfa, G.G., (2014). Synthesis and characterization of titanium oxidenano materials using sol-gel method. *Am. J. Nanosci. Nanotechnol*, **2**(1), pp.1-7.
13) Karunakaran, C., Senthilvelan, S., Karuthapandian, S., (2004). Photo oxidation of iodide ion on some semiconductor and non-semiconductor surfaces. *Catalysis Communications*, **5**(6), pp. 283 - 290. https://doi.org/10.1016/j.catcom.2004.03.002
14) Latroche, M., Brohan, L., and Tournoux, M., (1989). New holl and iteoxides: TiO2 (H) and K0. 06TiO2. *Journal of Solid State Chemistry*, **81**(1), pp.78-82. https://doi.org/10.1016/0022-4596(89)90204-1
15) Liu, B., Wen, L. and Zhao, X., (2007). The photoluminescence spectroscopic study of anatase TiO2 prepared by magnetron sputtering. *Materials Chemistry and Physics*, **106**(2-3), pp.350-353. https://doi.org/10.1016/j.matchemphys.2007.06.012
16) Ohenoja, K., Illikainen, M. and Niinimäki, J., (2013). Effect of operational parameters and stress energies on the particle size distribution of TiO2 pigment in stirred media milling. *Powder technology*, **234**, pp.91-96. https://doi.org/10.1016/j.powtec.2012.09.038

17) Qu, X., Alvarez, P.J. and Li, Q., (2013). Applications of nanotechnology in water and waste water treatment. *Water research*, **47**(12), pp.3931-3946. https://doi.org/10.1016/j.watres.2012.09.058

18) Rabeh, M.B., Khedmi, N., Fodha, M.A. and Kanzari, M., (2014). The effect of thickness on optical band gap and N-type conductivity of CuInS2 thin films a nealedinair atmosphere. *Energy Procedia*, **44**, pp.52-60. https://doi.org/10.1016/1350-4495(94)90026-4

19) Shamaila, S., Sajjad, A.K.L., Chen, F. and Zhang, J., (2010). Synthesis and characterization of mesoporous-TiO2 with enhanced photo catalytic activity for the degradation of chlorophenol. *Materials Research Bulletin*, **45**(10), pp.1375-1382. https://doi.org/10.1016/j.materresbull.2010.06.047

20) Sikorska, E., Khmelinskii, I.V., Bourdelande, J.L., (2003). Diffuse reflectance spectroscopy in photochemistry of opaque food products-methods and applications. *Polish journal of food and nutrition sciences*, **12**(Suppl. 2), pp.100-107.

21) Simons, P.Y. and Dachille, F.J.A.C., (1967). The structure of TiO2II, a high-pressure phase of TiO2. *Acta Crystallographica*, **23**(2), pp.334-336. https://doi.org/10.1107/S0365110X67002713

22) Su, C., Tseng, C.M., Chen, L.F., (2006). Sol–hydro thermal preparation and photo catalysis of titanium dioxide. *Thin Solid Films*, **498**(1-2), pp.259-265. https://doi.org/10.1016/j.tsf.2005.07.123

23) Uddin M, Uddin MM, and Khan MAH. (2021). Effect of shift parameters in rational Krylov subspace method for solving Riccati equations arise from power system models, *Int. J. Mat. Math. Sci*., **3**(2), 43-49. https://doi.org/10.34104/ijmms.021.043049

24) Wang, J., Mao, B., Gole, J.L., (2010). Visible-light-driven reversible and switch able hydrophobic to hydrophilic nitrogen-doped titanium surfaces: correlation with photo catalysis. *Nanoscale*, **2**(10), pp.2257-2261. https://doi.org/10.1039/C0NR00313A

25) Yousif AAA., and Ali EHM. (2021). Determination of piles bearing capacity using empirical methods and (AllPile 6) software -cases studies Portsudan and Khartoum cities, *Int. J. Mat. Math. Sci*., **3**(5), 113-121. https://doi.org/10.34104/ijmms.021.01130121

26) Zhu, Y., Zhang, L., Gao, C., & Cao, L. (2000). The synthesis of nano sized TiO2powder using a sol-gel method with TiCl4 as a precursor, *J. of Materials Science*, **35**(16), 4049-4054. https://doi.org/10.1023/A:1004882120249

Citation: Elrazeg YA, Badiruzzaman M, Islam M, Morshed MM, and Elmugdad AA. (2022). Synthesis of titanium dioxide by sol-gel method and comparison with titanium dioxide pure, *Int. J. Mat. Math. Sci.*, **4**(3), 75-82. https://doi.org/10.34104/ijmms.022.075082